Research Paper

Author for correspondence:
Hongcheng Zhou,
E-mail: zhouhc@home.swjtu.edu.cn

CAMBRIDGE UNIVERSITY PRESS

Design of multi-band and high radiation intensity piezoelectric antenna based on external circuit

Yong Zhang[1], Zhongming Yan[1,2], Biao Dong[1], Yu Wang[1,2]
and Hongcheng Zhou[1,2] (iD)

[1]School of Electrical Engineering, Southwest Jiaotong University, Chengdu 610000, China and [2]Key Laboratory of Magnetic Suspension Technology and Maglev Vehicle, Ministry of Education, Chengdu 610000, China

Abstract

This paper presents a novel method to improve the working bandwidth and radiation intensity of piezoelectric antenna by using external circuit. This method makes the piezoelectric antenna combined with roles of high radiation intensity and multiple resonant frequencies without changing the structural size of the piezoelectric antenna. The experimental results show that, compared with the original piezoelectric antenna, the tuning range of the resonant frequency of the piezoelectric antenna caused by the series capacitance and inductance is +13.6 and −24%, respectively. The series inductance will produce new resonance frequency, which provides a new method for the multi-band operation of the piezoelectric antenna. The LLC (series and parallel circuit) composite circuit can increase the number of resonant frequencies of the piezoelectric antenna from 1 to 3, and the S_{11} at the resonant frequencies are all lower than −10 dB, and the radiated magnetic field of the piezoelectric antenna is increased by 42.3% at least. This method makes the piezoelectric antenna have the dual functions of high radiation intensity and multi-band, which has great significance for broadening the application field of piezoelectric antenna.

Introduction

Low frequency (LF, 30–300 kHz) and lower frequency (<30 kHz) electromagnetic waves have long wavelength, which has the characteristics of long propagation distance and strong anti-electromagnetic pulse interference ability, and can achieve ultra-long propagation through the atmosphere. It is of great significance for transcontinental communication [1]. Compared with high-frequency electromagnetic waves, the low-frequency electromagnetic waves have less attenuation in seawater, which is of great significance for submarine communication [2]. The excellent penetration performance of low-frequency electromagnetic waves also plays an important role in the fields of through-the-earth communication and geological survey [3]. Among many applications, the application of submarine underwater communication is the most prominent, which can solve the problem of long-distance and large-depth communication between the communication base station and the submarine. For example, the very low frequency transmitter station built in Rosnay, France, with a working frequency of 15.1∼21.7 kHz, can realize submarine communication in a water depth of 10 m. In 1961, the Cutler very low frequency antenna was built in Cutler, Maine, USA, with an operating frequency of 14∼30 kHz, and its mission was the underwater communication of submarines in the Atlantic Ocean [4]. The ultra-low frequency communication system developed by the "Sanguine" program and the "Seafarer" program can realize deep-water submarine communication on a global scale.

In order to make the LF antenna effectively radiate electromagnetic waves, the size of the LF antenna usually needs to reach $\lambda_0/10$ or more, which is an unbearable physical size for wireless communication systems, and is accompanied by high construction costs and high power consumption [5, 6]. At present, the LF communication systems that have been built are huge, and their size is in the order of tens of kilometers, which will cause the antenna system easy to be found and destroyed [7]. In order to solve the above problems, the acoustic strain powered antenna can decouple the antenna size from the electromagnetic wave wavelength. Even at a very low frequency, the antenna can still maintain small volume level, and there is no complex impedance matching network. It has broad application prospects in the fields of transcontinental communication, submarine communication and through-the-earth communication.

Acoustic strain powered antenna is based on the dynamic coupling between acoustic wave and electromagnetic wave inside ferroelectric or ferromagnetic materials to realize the conversion between mechanical energy and electromagnetic energy, and the electromagnetic radiation is generated. It is divided into piezoelectric antenna and magnetoelectric antenna

according to different working principles [8–11]. Acoustic strain powered antenna has the advantages of small volume, easy integration and simple impedance matching network. It has broad application prospects in the fields of miniature brain implants, energy harvesting, underwater communications and medical devices [12–15]. At present, the development of communication technology based on acoustic strain powered antenna is inadequate. In practical applications, it is necessary to improve its radiation intensity and operating bandwidth to enhance the environmental adaptability of acoustic strain powered antenna. The resonant frequency and radiation intensity of the acoustic strain powered antenna will change with the size and material type of piezoelectric material, which will increase the design complexity and make integration difficult. Therefore, it is of great significance to find a technical solution that takes into account both the radiation efficiency and the bandwidth without changing the acoustic strain powered antenna structure.

In order to improve the radiation intensity and working bandwidth of the acoustic strain powered antenna, many scholars have carried out some research, which mainly includes acoustic strain powered antenna array technology, acoustic strain powered antenna modulation technology, material selection of acoustic strain powered antenna, changing the size of the acoustic strain powered antenna, and designing acoustic strain powered antenna electrode with different areas. In [16], the magnetoelectric antenna with a new structure was proposed. A nanomagnetic array with magnetostrictive effect was deposited on the surface of piezoelectric substrate. The oscillating magnetizations of nanomagnetic array radiate electromagnetic wave at the frequency of the surface acoustic wave (SAW). This new structure can produce high radiation intensity. In [17], the method of using series and parallel antenna array to improve magnetoelectric antenna gain and bandwidth was discussed, and the array magnetoelectric antenna has broad application prospects in the field of biological implantable. In [18], the direct antenna modulation (DAM) was applied to the very low frequency magnetoelectric antenna, and the farthest communication distance was 120 m. In [19], the ultra-low loss lithium niobate (LiNbO3) crystal was used as the radiator of the piezoelectric antenna. At the same frequency, the radiation efficiency was more than 300 times higher than that of the dipole antenna with the same size. The modulation bandwidth is 83 times higher than the traditional Bode-Fano limit by using DAM. In [20], in order to enhance the radiation intensity of piezoelectric antenna, the LiNbO3 piezoelectric crystal was replaced by lead zirconate titanate (PZT) piezoelectric ceramic. Compared with piezoelectric crystals, the piezoelectric ceramics have higher piezoelectric strain constant and dielectric constant. The surrounding air medium was not easy to be broken down, and has higher radiation intensity. In [21], the relationship between the resonant frequency of magnetoelectric antenna and the size of piezoelectric material was studied. The resonant frequency is inversely proportional to the thickness and width of piezoelectric material. The magnetoelectric antennas can operate at different resonant frequencies by changing the size of piezoelectric material, which provides a new method for the realization of broadband of magnetoelectric antenna. In [22], the electromagnetic radiation mechanism and PZT piezoelectric antenna characterization were discussed in terms of the material and structure. The resonant frequency was adjusted by the radius and height of the PZT antenna. According to different materials and structural parameters, the piezoelectric metamaterial antenna was designed for multi-band and the improvement of electromagnetic radiation.

In summary, many researchers have paid great attention to the broadband and high radiation characteristics of acoustic strain powered antenna. In the existing solutions, the antenna array technology will increase the device complexity and need to consider the matching between units. The design scheme of changing the antenna material and size requires replacement antennas with different sizes and materials, which is impractical in applications. Therefore, it is of great significance to improve the bandwidth and radiation intensity of the piezoelectric antenna without changing the structure and size of the antenna.

In this paper, we improve the working bandwidth and radiation intensity of piezoelectric antenna based on inductance, capacitance and their composite circuit structure, and this method only need to adjust the inductance or capacitance values of the external circuit without changing the structure of the piezoelectric antenna. Firstly, the impedance characteristics of piezoelectric antenna are studied based on the Modified Butterworth-van Dyke (MBVD) equivalent circuit model, and the changing mechanism of radiation intensity and resonant frequency of piezoelectric antenna is revealed. Secondly, the experimental test platform is built to study the influences of series inductance and capacitance on the resonant frequency of piezoelectric antenna, and the variation regulation of series inductance and capacitance on the resonant frequency of piezoelectric antenna is obtained. Finally, the LLC external circuit with improved radiation intensity and resonant frequency of piezoelectric antenna is designed, and the experimental test is carried out. It is worth noting that the method proposed can be extended to other types of acoustic strain powered antenna. The design can effectively broaden the working bandwidth and enhance radiation intensity of piezoelectric antenna, which is of great significance for the application of piezoelectric antenna in low-frequency wireless communication system.

Theoretical analyses

Theoretical analysis of enhanced radiation intensity of piezoelectric antenna

The piezoelectric antenna structure includes electrodes and substrates. Not only the dielectric loss and mechanical vibration loss caused by the piezoelectric material itself cannot be ignored, but also the electrode loss and connection loss with the RF interface cannot be ignored. Therefore, the MBVD equivalent circuit model [23, 24] considering the losses is used for theoretical analysis of piezoelectric antenna, as shown in Fig. 1(a). Where C_m, L_m, R_m are motional capacitance, motional inductance and motional resistance respectively; R_0 represents dielectric loss in the piezoelectric materials; R_s represents electrode loss and lead wire loss; C_0 is a static capacitance, which represents the dielectric characteristics of the piezoelectric antenna [25].

The equivalent electrical impedance of the piezoelectric antenna is calculated according to Fig. 1(a):

$$
\begin{aligned}
Z_{in} &= R_s + \left(\frac{1}{j\omega C_m} + j\omega L_m + R_m \right) // \left(R_0 + \frac{1}{j\omega C_0} \right) \\
&= R_s + \left[\frac{1}{R_0 + \frac{1}{j\omega C_0}} + \frac{1}{R_m + j\left(\omega L_m - \frac{1}{\omega C_m} \right)} \right]^{-1} \\
&= R_s + \left[(R_0 + j\omega C_0) + \frac{j\omega C_m}{1 - \omega^2 C_m L_m + j\omega C_m R_m} \right]^{-1}
\end{aligned}
\tag{1}
$$

When the resonance occurs on the C_m, L_m, R_m branches in Fig. 1(a), the whole circuit becomes that the resistance R_m is connected in parallel with the capacitor C_0. At this time, the inductance L_{add-1} is connected in series, and the whole circuit is changed from parallel circuit to series circuit. The inductance L_{add-1} can effectively offset the capacitive part generated by C_0 in the circuit, and can also generate a new resonant frequency with C_0. In addition, when the L and C series circuit is connected in parallel with piezoelectric antenna, the inductive reactance is very small and the capacitive reactance is very large. The transmission loss of piezoelectric antenna is very small. Therefore, based on Fig. 1 (a), the parallel LC circuit and the series variable inductance are used to regulate the radiation intensity and resonant frequency of the piezoelectric antenna. The equivalent circuit is shown in Fig. 1(b), which is called LLC circuit.

The equivalent electrical impedance of the piezoelectric antenna is calculated according to Fig. 1(b):

$$
\begin{aligned}
Z_{in} =& R_s + \left(\frac{1}{j\omega C_m} + j\omega L_m + R_m\right) // \left(R_0 + \frac{1}{j\omega C_0}\right) // \left(\frac{1}{j\omega C_{add}} + j\omega L_{add-2}\right) + j\omega L_{add-1} \\
=& R_s + \left[\frac{1}{\frac{1}{j\omega C_m} + j\omega L_m + R_m} + \frac{1}{R_0 + \frac{1}{j\omega C_0}} + \frac{1}{\frac{1}{j\omega C_{add}} + j\omega L_{add-2}}\right]^{-1} + j\omega L_{add-1}
\end{aligned}
\tag{2}
$$

By comparing equations (1) and (2) can be seen that, it is necessary to realize the impedance transformation of the piezoelectric antenna by the matching network. The impedance of the piezoelectric antenna is changed to make it close to the output impedance, so as to achieve the best power transmission matching. On the other hand, the impedance of the piezoelectric antenna is adjusted by inductive components, and the phase angle of impedance tends to zero at the resonant frequency. The reactive component of transmission power is reduced and the transmission efficiency of piezoelectric antenna is enhanced.

Theoretical analysis of resonant frequency variation of piezoelectric antenna

In order to meet the needs of modern wireless communication systems, the antennas must develop in the direction of miniaturization, multi-function and high performance. In many cases, a wireless communication device needs to work in multi-band, so as to simplify the design of the communication system and reduce the cost. In order to solve the problem, multi-band antenna becomes the preferred solution. The advantage of multi-band antennas is that a single antenna can achieve the performance of multiple antennas. In practical applications, the wireless communication system utilizes multi-band combination of antennas, which has good working performance. Especially in dealing with various complex environments, it has obvious advantages.

At present, one of the challenges of piezoelectric antennas is that their operating bandwidth is narrow, which only has the best performance at the resonant frequency. The design of multi-band performance can broaden the operating frequency of piezoelectric antennas to deal with various complex application environments.

The MBVD model of the original piezoelectric antenna in Fig. 1(a) includes series resonant branches and parallel resonant branches, which cause the series resonant frequency and parallel resonant frequency of the piezoelectric antenna respectively. It is worth noting that the working frequency of the piezoelectric antenna is at the series resonant frequency, so the proposed
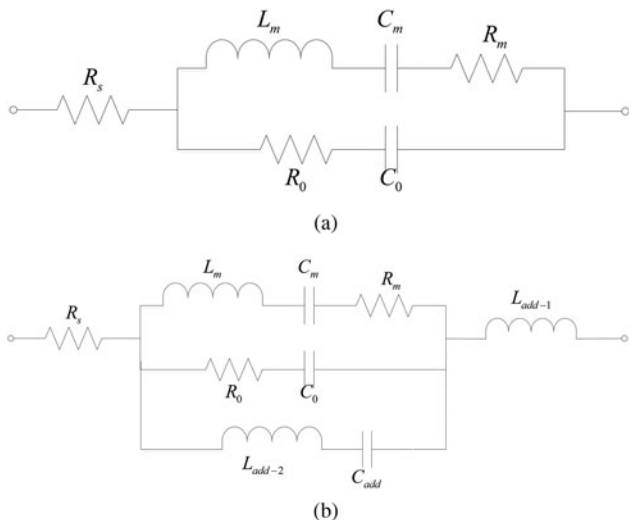

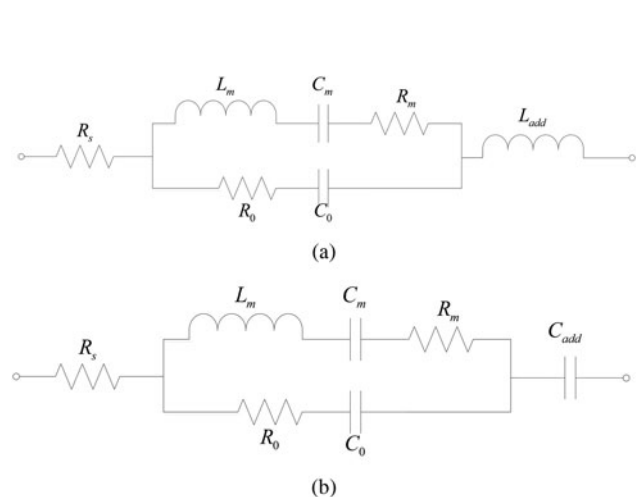**Fig. 1.** (a) MBVD equivalent circuit model. (b) LLC matching circuit.

Fig. 2. (a) Equivalent circuit of piezoelectric antenna with series inductance. (b) Equivalent circuit of piezoelectric antenna with series capacitance.

method is mainly to change the series resonant frequency of the piezoelectric antenna. The tunable circuit is designed based on the equivalent circuit of piezoelectric antenna, which is connected in series with inductance or capacitance respectively, as shown in Fig. 2.

The series resonance frequency f_s and parallel resonance frequency f_p are calculated in equivalent circuit of Fig. 1(a):

$$f_s = \frac{1}{2\pi\sqrt{L_m C_m}}$$

$$f_p = \frac{1}{2\pi\sqrt{\dfrac{L_m C_m C_0}{C_m + C_0}}} \quad (3)$$

The series resonance frequency f_s and parallel resonance frequency f_p are calculated in equivalent circuit of Fig. 2(a):

$$f_s = \frac{1}{2\pi\sqrt{(L_m + L_{add})C_m}}$$

$$f_p = \frac{1}{2\pi\sqrt{\dfrac{L_m C_m C_0}{C_m + C_0}}} \quad (4)$$

The series resonance frequency f_s and parallel resonance frequency f_p are calculated in equivalent circuit of Fig. 2(b):

$$f_s = \frac{1}{2\pi\sqrt{L_m\left(\dfrac{C_m C_{add}}{C_m + C_{add}}\right)}}$$

$$f_p = \frac{1}{2\pi\sqrt{\dfrac{L_m C_m C_0}{C_m + C_0}}} \quad (5)$$

By comparing equations (3)–(5), it can be seen that when the series resonance is occurred in the series resonance branch, the series inductance increases the equivalent inductance of the whole circuit. The series inductance will cause the f_s to shift to the low frequency, and the f_p remains unchanged. In addition, the series inductance interacts with the inherent capacitance C_0, which can generate new resonant frequency. When the series resonance is occurred in the series resonance branch, the series capacitance reduces the equivalent capacitance of the whole circuit. The series capacitance will cause the f_s to shift to the high frequency, and the f_p remains unchanged. Because the series
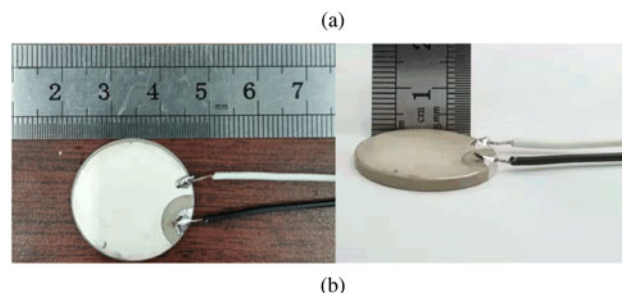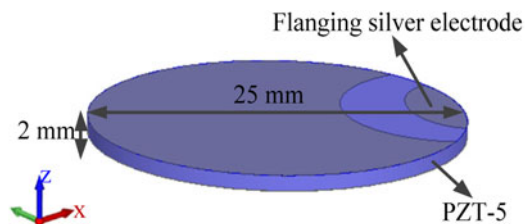

Fig. 3. (a) Schematic diagram of the piezoelectric antenna. (b) Prototype picture of the piezoelectric antenna.

capacitance and the inherent capacitance C_0 are capacitive, no new resonant frequency is generated.

Design and fabrication of piezoelectric antenna

In order to analyze the radiation performance and resonant frequency of piezoelectric antenna, a disk-type piezoelectric antenna is designed, as shown in Fig. 3. The material is composed of PZT-5 with diameter of 25 mm and height of 2 mm, and its polarization direction is along the thickness direction. The top and bottom of PZT-5 disk are plated with 20 μm flanging silver electrode. The flanging electrode can facilitate the welding of lead wires. The two wires are welded to the top and bottom silver electrodes of the PZT disk to provide electrical excitation.

The COMSOL Multiphysics finite element software is used to simulate the resonant frequency, stress and displacement of the piezoelectric antenna. The simulation result is shown in Fig. 4. It can be seen from Fig. 4 that the resonant frequency of the piezoelectric antenna is 79 kHz. At the resonant frequency, the maximum stress of the piezoelectric antenna is 46 kPa, which is distributed in the center of the piezoelectric antenna. The maximum displacement of piezoelectric antenna is 3.6×10^{-6} mm, and it is mainly distributed on the edge of the piezoelectric antenna. The center of the piezoelectric antenna has the lowest
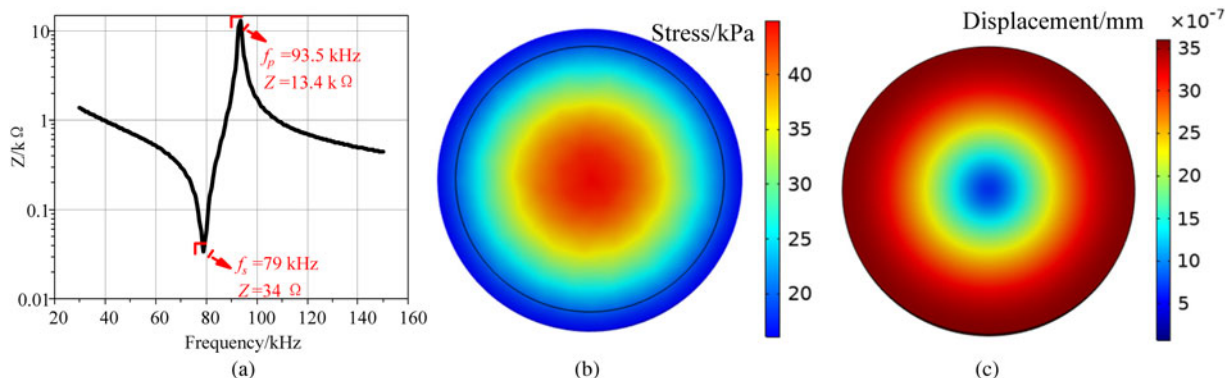

Fig. 4. (a) FEM calculates the resonant frequency. (b) Stress distribution at resonant frequency. (c) Displacement distribution at resonant frequency.
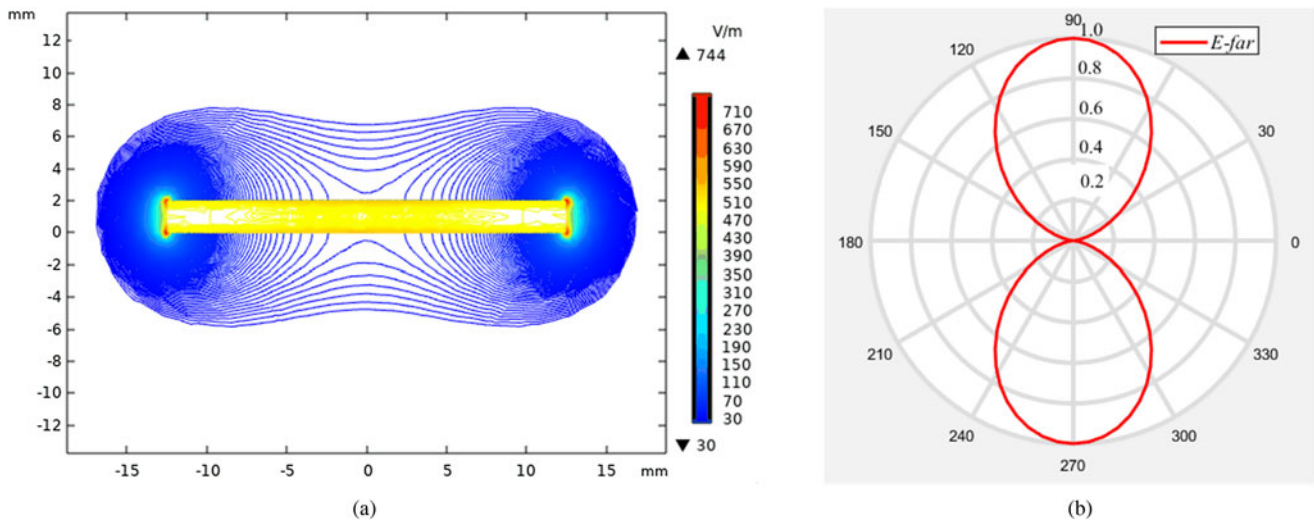
Fig. 5. (a) Near-field radiation pattern. (b) Normalized far-field radiation pattern.

amount of displacement. From the displacement distribution in Fig. 4(c), it can be seen that the vibration pattern of the piezoelectric antenna is radial vibration.

In addition, the radiation pattern of the original piezoelectric antenna is analyzed, as shown in Fig. 5. Figure 5(a) shows the electric field distribution of the near field of the piezoelectric antenna simulated by COMSOL, and Fig. 5(b) shows the electric field distribution of the far field of the piezoelectric antenna obtained by using the near-far field transformation theory [26]. From the electric field distribution of the near-field and far-field of the original piezoelectric antenna in Fig. 5, it can be seen that the radiation pattern of the piezoelectric antenna is equivalent to the electric dipole [27].

Fig. 6. (a) The sketch of the analog inductor. (b) The prototype of the analog inductance.

Experimental researches

Design and fabrication of variable inductance

The distributed capacitance and internal resistance in the real inductance greatly weaken the performance of piezoelectric antenna. The inductances with different values need to be replaced to adjust the resonant frequency of the piezoelectric antenna, and the variation of resonant frequency is discontinuous. In order to solve the above problems, the analog inductance can be realized by using a synthetic circuit [28], whose sketch is shown in Fig. 6(a).

$$L = \frac{R_1 R_3 R_4 C_1}{R_2} \tag{6}$$

The analog inductance consists of three constant resistors R_1, R_2 and R_3, an adjustable resistor R_4, a capacitor C_1 and two OPA445AP operational amplifiers [29]. The equivalent inductance of this circuit is calculated by equation (6) [30], and the inductance value L can be adjusted by selecting appropriate R_4. The adjustable range of equivalent inductance L is 0~20 mH in Fig. 6(b).

Experimental platform construction

The experimental test platforms are established to test the resonant frequency and radiation intensity of the piezoelectric antenna with external circuit. The experimental platforms are shown in Fig. 7. Figure 7(a) is the test schematic diagram for transmission distance and radiation magnetic field of piezoelectric antenna. Firstly, the sine wave signal is generated by the signal generator, which is amplified by the power amplifier and then loaded into the piezoelectric antenna to generate electromagnetic waves. The electromagnetic wave is received by the copper coil and transmitted to the oscilloscope to display in the form of voltage. The copper coil is made of enameled wire with a diameter of 0.35 mm, and the number of turns is 1000. According to the electromagnetic induction principle, the induced voltage of the copper coil is proportional to the magnitude of the alternating magnetic field. The unknown alternating magnetic field can be calculated by measuring the output voltage of the copper coil. Figure 7(b) is
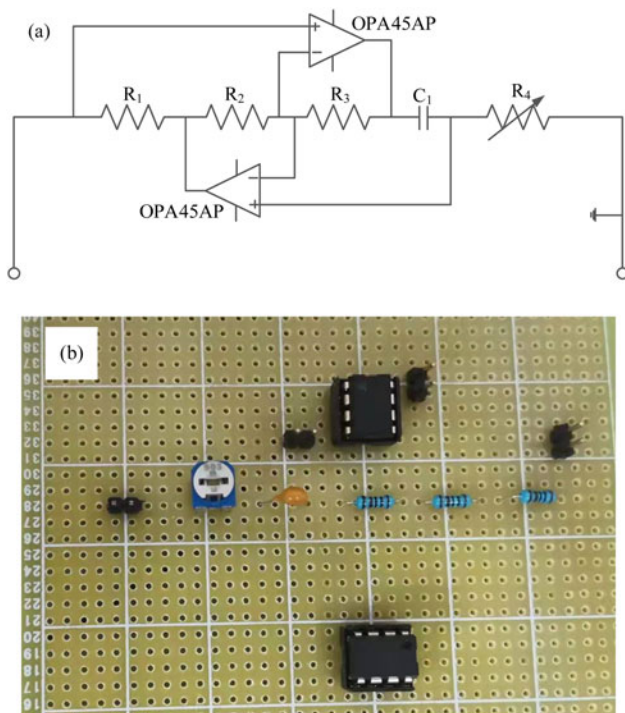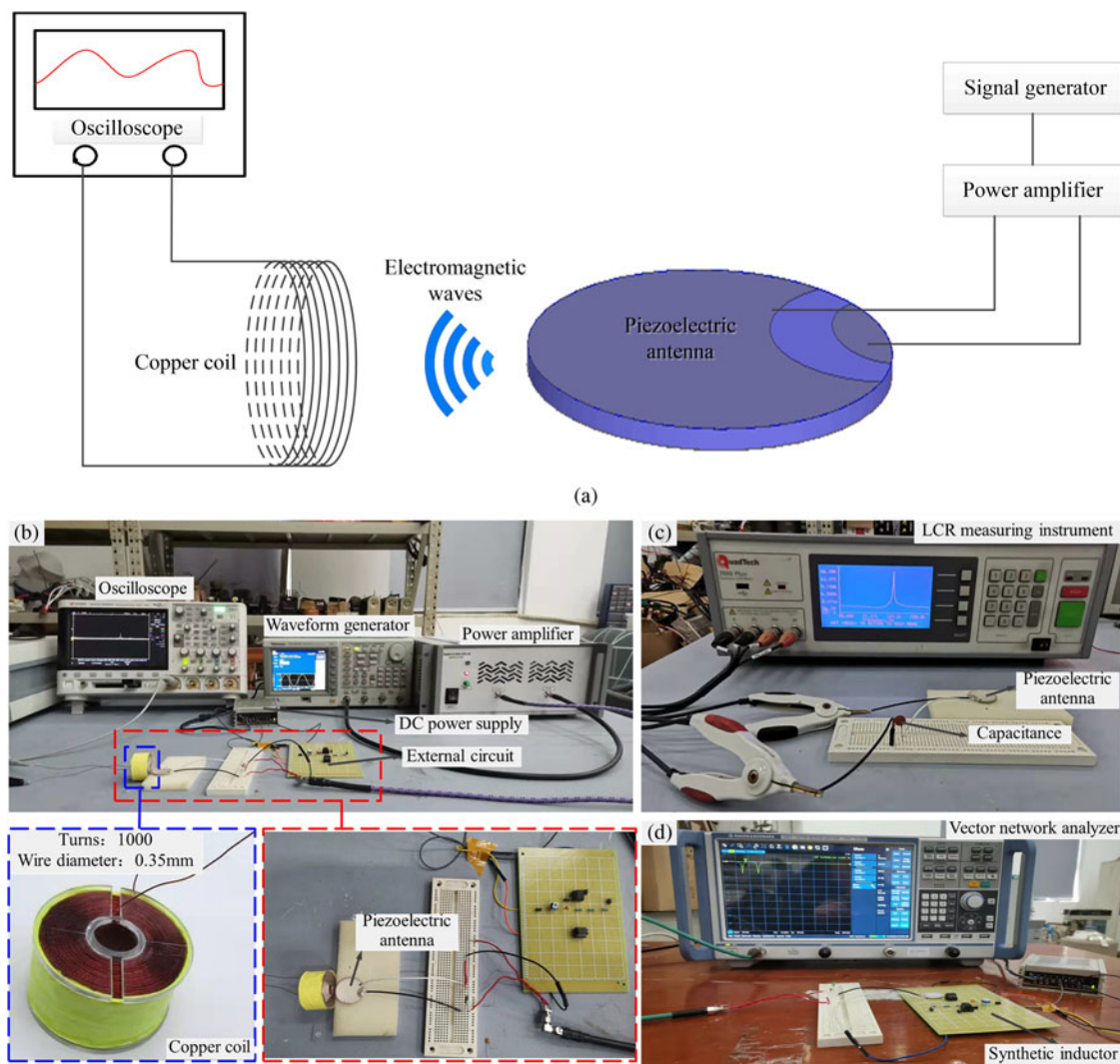
Fig. 7. (a) Electromagnetic radiation test schematic diagram. (b) Electromagnetic radiation test platform. (c) Impedance test platform. (d) S-parameter test platform.

the test platform for transmission distance and radiation magnetic field of piezoelectric antenna and the experimental equipment is composed of signal generator (Tektronix AFG3252C), oscilloscope (Keysight InfiniiVision MSQX3024T), power amplifier, copper coil. Figure 7(c) is the test platform for resonant frequency and impedance characteristics of piezoelectric antenna and the experimental equipment is the Precision LCR Meter produced by QuadTech Company. Figure 7(d) is the test platform for S-parameter of piezoelectric antenna and the experimental equipment are the vector network analyzer (Rohde & Schwarz®ZNB8-B34) and coaxial cable.

Experimental study on piezoelectric antenna tuning

Based on the analysis of tuning mechanism in section 'Theoretical analyses', the piezoelectric antenna with the series inductance and capacitance are tested in Fig. 7(c) and the test results are shown in Fig. 8.

It can be seen from Fig. 8(a) that the series capacitance will cause the series resonance frequency to shift to high frequency, while the parallel resonance frequency remains unchanged. The resonant frequency of the original piezoelectric antenna is 78.6 kHz. The piezoelectric antenna is connected in series with a 1.5 nF capacitance, and the resonant frequency is 89.3 kHz, which increases by 13.6%. The piezoelectric antenna is connected in series with a 2.2 nF capacitance, and the resonant frequency is 86.4 kHz, which increases by 10%. It can be seen from Fig. 8(b) that the series inductance will cause the series resonant frequency to shift to low frequency, while the parallel resonance frequency remains unchanged. The piezoelectric antenna is connected in series with a 1.7 mH inductance, and the resonant frequency is 59.7 kHz, which is reduced by 24% compared with the original piezoelectric antenna. With the increase of series inductance, the series resonant frequency decreases. When the series inductance of the piezoelectric antenna increases by 7.7 times, the series resonant frequency decreases by 22.4%. In addition, the series inductance interacts with the inherent capacitance C_0, which can generate new resonant frequency. The piezoelectric antenna is connected in series with a 1.7 mH inductance, and the new resonant frequency is 113.1 kHz, which is increased by 44% compared with the original piezoelectric antenna. Compared with Figs 8(a) and 8(b), it can be found that the series inductance
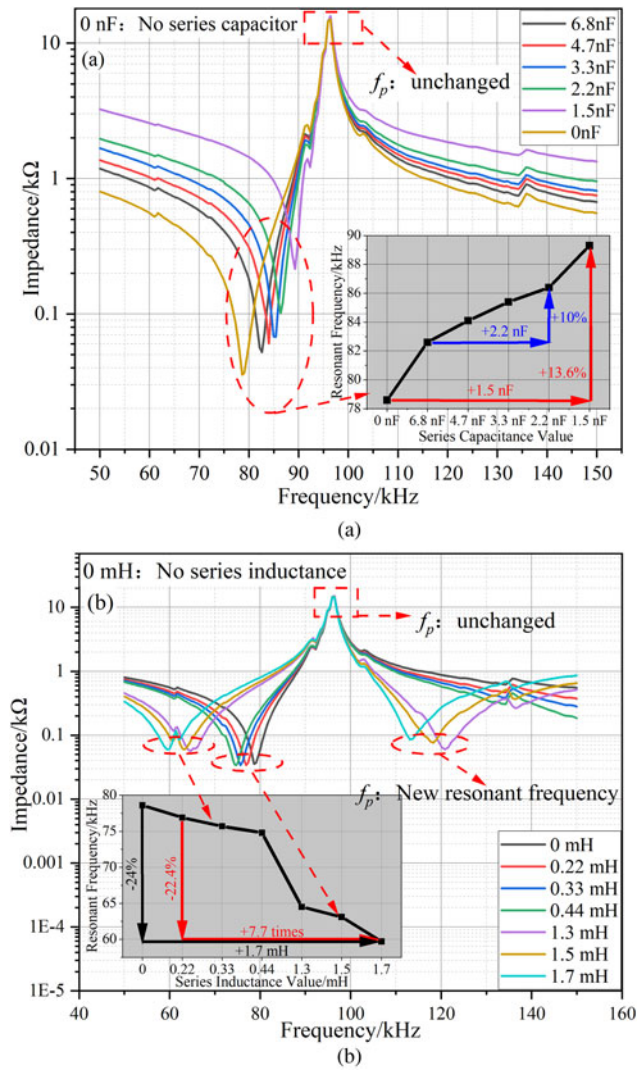
Fig. 8. (a) Influence of series capacitance on resonant frequency of piezoelectric antenna. (b) Influence of series inductance on resonant frequency of piezoelectric antenna.

Fig. 9. (a) The matching diagram of LLC circuit and piezoelectric antenna. (b) The S_{11} parameters of the piezoelectric antenna. (c) The radiated magnetic fields at the three resonant frequencies.

has more than significant effect on the series resonant frequency of piezoelectric antenna. The series inductance will generate a new resonant frequency, while the series capacitor will not generate a new resonant frequency.

In summary, the resonant frequency of the piezoelectric antenna can be effectively adjusted by the series inductance or capacitance without changing the structure of the piezoelectric antenna, which broadens the working bandwidth of the piezoelectric antenna. On the other hand, the new resonant frequency is generated by series inductance, which can make the piezoelectric antenna work at multi-band, and further broaden the application field of piezoelectric antenna.

Experimental study on improving radiation intensity of piezoelectric antenna

Based on the theoretical analysis of improving radiation intensity of piezoelectric antenna in section 'Theoretical analyses', the piezoelectric antenna with the external LLC matching circuit is tested in Figs 7(b) and 7(d), and the test results are shown in
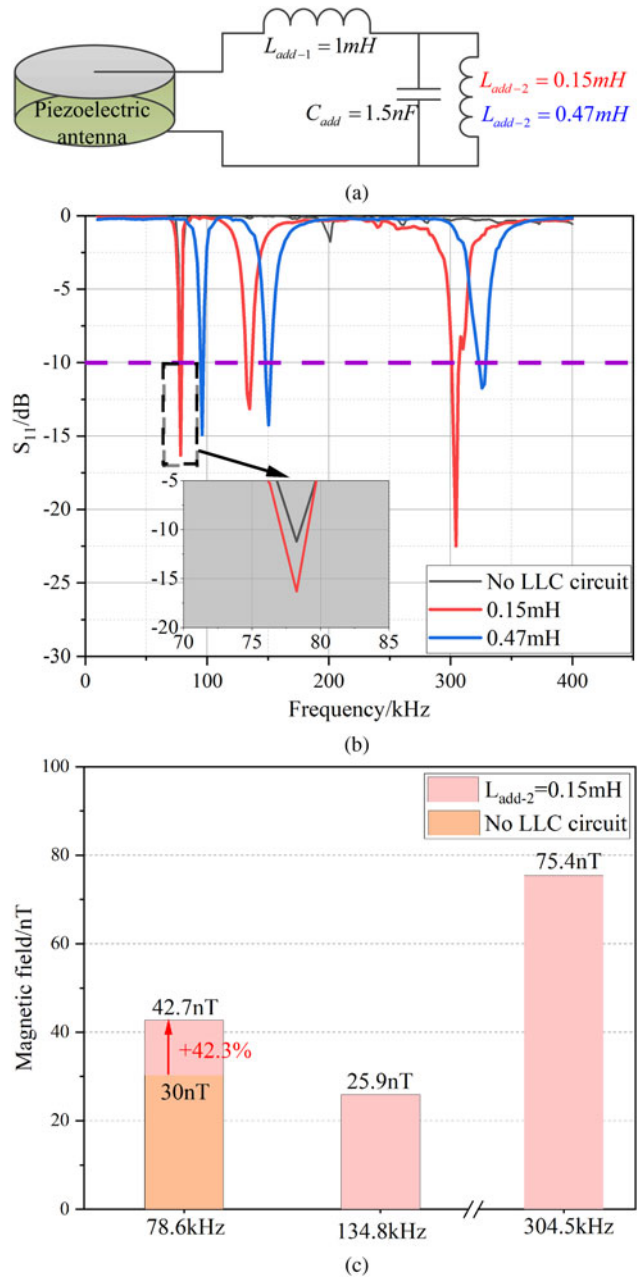
Fig. 9. The matching diagram of LLC circuit and piezoelectric antenna is shown in Fig. 9(a). The series inductance L_{add-1} and parallel capacitance C_{add} are constant, which are 1 mH and 1.5 nF respectively. The parallel inductance L_{add-2} is an adjustable analog inductance, as shown in Fig. 6(b). The resonant frequency and radiation intensity of piezoelectric antenna are adjusted by setting different L_{add-2}. In this section, the parallel inductance L_{add-2} with 0.15 and 0.47 mH is taken as an example to contrastive analysis the influence of LLC circuit with different L_{add-2} on the resonance frequency and radiation intensity of the piezoelectric antenna.

The S_{11} parameters of the piezoelectric antenna measured by vector network analyzer with or without an external LLC circuit

are showed in Fig. 9(b). As can be seen from Fig. 9(b), when the piezoelectric antenna without external LLC circuit, the piezoelectric antenna has only one resonant frequency at 78.6 kHz, and S_{11} is −11.2 dB. When the piezoelectric antenna with LLC matching circuit and L_{add-2} is 0.15 mH, the piezoelectric antenna has three resonant frequency, which are 78.6, 134.8 and 304.5 kHz respectively, and the S_{11} at the resonant frequencies are all lower than −10 dB. When the piezoelectric antenna with LLC matching circuit and L_{add-2} is 0.47 mH, the piezoelectric antenna also has three resonant frequency, which are 95.8, 150.4 and 325.9 kHz respectively, and the S_{11} at the resonant frequencies are all lower than −10 dB. Compared with the no external LLC circuit, the resonant frequency of the piezoelectric antenna with LLC circuit is increased to three, and the radiation intensity of the piezoelectric antenna is also greatly improved. The piezoelectric antenna has the dual functions of multi-band and the improvement of electromagnetic radiation.

In order to verify the effectiveness of multi-band of the piezoelectric antenna with LLC circuit, the radiated magnetic field of the three resonant frequencies of the piezoelectric antenna is analyzed when the piezoelectric antenna with the LLC circuit and the L_{add-2} is 0.15 mH. The test results are obtained from the test platform in Fig. 7(b). The distance between the piezoelectric antenna and the receiving cooper coil is constant, which is 10 cm. The radiated magnetic fields at the three resonant frequencies are obtained, as shown in Fig. 9(c). As can be seen from Fig. 9(c), compared with the original piezoelectric antenna, at the common resonant frequency of 78.6 kHz, the radiation magnetic field of the piezoelectric antenna with the LLC circuit is 42.3% higher. In addition, when the piezoelectric antenna with the LLC circuit, the two new resonance frequencies are 134.8 and 304.5 kHz, respectively, and the radiated magnetic fields are 25.9 and 75.4 nT, respectively. In summary, when the piezoelectric antenna is connected with LLC circuit, it can not only make the piezoelectric antenna work at multi-band, but also enhance the electromagnetic radiation of the piezoelectric antenna.

Conclusion

In this paper, a new design method of piezoelectric antenna with high radiation intensity and multi-band is proposed and verified by experiments. By adjusting the inductance or capacitance of the external circuit, the radiation intensity and resonant frequency of the piezoelectric antenna are adjusted without changing the structure of the piezoelectric antenna. The impedance characterization of piezoelectric antenna is studied based on MBVD model, and the variation mechanism of multi-band and the enhancement of radiation intensity of piezoelectric antenna are revealed, which provides theoretical basis for the design of piezoelectric antenna. The influence of piezoelectric antenna with series inductance or capacitance on the resonant frequency is analyzed. The experimental results show that the series capacitance will cause the series resonant frequency to shift to high frequency, and the series inductance will cause the series resonant frequency to shift to low frequency. Comparison with the original piezoelectric antenna, the tuning range of the series capacitance and inductance on the resonant frequency of piezoelectric antenna is +13.6 and −24% respectively. The new resonant frequency is generated by series inductance and inherent capacitance C_0, which is of great significance to the multi-band operation of the piezoelectric antenna. The LLC composite circuit can increase the resonant frequency of the piezoelectric antenna from 1 to 3,

and the S_{11} at the resonant frequencies are all lower than −10 dB, and the radiated magnetic field of the piezoelectric antenna is increased by 42.3% at least. It has dual functions of high radiation intensity and multi-band operation. This method is of great significance for broadening the application field and improving the transmission distance of piezoelectric antenna.

Data

The data that support the findings of this study are available from the corresponding author upon reasonable request.

Conflict of interest. The authors declare that they have no known conflict of interest or personal relationships that could have appeared to influence the work reported in this paper.

References

1. **Pelosi G, Selleri S and Valotti B** (2004) From Poldhu to the Italian station of Coltano: Marconi and the first years of transcontinental wireless. *IEEE Antennas and Propagation Magazine* **46**, 47–54.
2. **Guo DR, Lu H and Chen Y** (2011) The feasibility analysis of shipborne ULF/VLF submarine communication. *Chinese Journal of Radio Science* **26**, 1148–1152.
3. **Sun Z and Akyildiz IF** (2010) Magnetic induction communications for wireless underground sensor networks. *IEEE Transactions on Antennas and Propagation* **7**, 2426–2435.
4. **Mao ZW, Gao C, Lu F and Su LY** (2012) Radiation environment analysis of the United States of America submarine transmitting station at Cutler. in *2012 6th Asia-Pacific Conference on Environmental Electromagnetics (CEEM). IEEE, Shanghai, China*, pp. 376–380.
5. **Madanayake A, Choi S, Tarek M, Dharmasena S, Mandal S, Glickstein J and Sehirlioglu A** (2017) Energy-efficient ULF/VLF transmitters based on mechanically-rotating dipoles. *2017 Moratuwa Engineering Research Conference(MERCon). IEEE, Moratuwa, Sri Lanka*, pp. 230–235.
6. **Sinha D and Amaratunga G** (2015) Electromagnetic radiation under explicit symmetry breaking. *Physical Review Letters* **14**, 147701.
7. **Sojdehei JJ, Wrathall PN and Dinn DF** (2001) Magneto-inductive (MI) communications. *MTS/IEEE Oceans 2001. An Ocean Odyssey. Conference Proceedings (IEEE Cat. No.01CH37295). IEEE, Honolulu, HI, USA*, vol. 1, pp. 513–519.
8. **Xu G, Xiao S, Li Y and Wang B** (2021) Modeling of electromagnetic radiation induced from a magnetostrictive/piezoelectric laminated composite. *Physics Letters A* **385**, 126959.
9. **Xu J, Leung CM, Zhuang X, Li J, Bhardwaj S and Volakis J** (2019) A low frequency mechanical transmitter based on magnetoelectric heterostructures operated at their resonance frequency. *Sensors* **19**, 853.
10. **Cao J, Yao H, Pang Y, Xu J, Lan C and Lei M** (2022) Dual-band piezoelectric artificial structure for very low frequency mechanical antenna. *Advanced Composites and Hybrid Materials* **5**, 410–418.
11. **Zhang Y, Yan ZM, Han TH, Zhu SS, Wang Y and Zhou HC** (2022) Design of a low-frequency miniaturized piezoelectric antenna based on acoustically actuated principle. *Chinese Physics B* **7**, 077702.
12. **Kim S, Adib MR and Lee K** (2019) Development of chipless and wireless underground temperature sensor system based on magnetic antennas and SAW sensor. *Sensors and Actuators A: Physical* **157**, 1–6.
13. **Martos-Repath I, Mittal A and Zaeimbashi M** (2020) Modeling of magnetoelectric antennas for circuit simulations in magnetic sensing applications. *IEEE 63rd International Midwest Symposium on Circuits and Systems (MWSCAS). IEEE, Springfield, MA, USA*, pp. 49–52.
14. **Nasrollahpour M, Romano A, Sun N and Zaeimbashi M** (2021) Magnetoelectric antenna for miniaturized acoustic noise dosimetry applications. *IEEE Sensors Letters* **5**, 2500704.

15. **Singer A, Dutta S, Lewis E, Chen Z, Chen JC and Verma N** (2020) Magnetoelectric materials for miniature, wireless neural stimulation at therapeutic frequencies. *Neuron* **107**, 631–646.

16. **Drobitch JL, De A, Dutta K, Pal PK, Adhikari A and Barman A** (2020) Extreme subwavelength magnetoelastic electromagnetic antenna implemented with multiferroic nanomagnets. *Advanced Materials Technologies* **5**, 2000316.

17. **Zaeimbashi M, Lin H, Dong C, Liang X, Nasrollahpour M and Chen H** (2019) NanoNeuroRFID: a wireless implantable device based on magnetoelectric antennas. *IEEE Journal of Electromagnetics, RF and Microwaves in Medicine and Biology* **3**, 206–215.

18. **Dong C, He Y, Li M, Tu C, Chu Z and Liang X** (2020) A portable very low frequency (VLF) communication system based on acoustically actuated magnetoelectric antennas. *IEEE Antennas and Wireless Propagation Letters* **19**, 398–402.

19. **Kemp MA, Franzi M, Haase A, Jongewaard E, Whittaker MT and Kirkpatrick M** (2019) A high Q piezoelectric resonator as a portable VLF transmitter. *Nature Communications* **10**, 1715.

20. **Hassanien AE, Breen M, Li M and Gong S** (2020) Acoustically driven electromagnetic radiating elements. *Scientific Reports* **10**, 17006.

21. **Nan TX, Lin H and Gao Y** (2017) Acoustically actuated ultra-compact NEMS magnetoelectric antennas. *Nature Communications* **8**, 296.

22. **Xu JC, Cao JQ and Guo MH** (2021) Metamaterial mechanical antenna for very low frequency wireless communication. *Advanced Composites and Hybrid Materials* **4**, 761–767.

23. **Jin H, Dong SR, Luo JK and Milne WI** (2011) Generalised Butterworth-Van Dyke equivalent circuit for thin-film bulk acoustic resonator. *Electronics Letters* **47**, 424–425.

24. **Vorobiev A and Gevorgian S** (2013) Enhanced tunable performance of high Q-factor BaxSr1-xTiO3 film bulk acoustic wave resonators. *International Journal of Microwave and Wireless Technologies* **5**, 361–369.

25. **Muralt P, Conde J, Artieda A, Martin F and Cantoni M** (2009) Piezoelectric materials parameters for piezoelectric thin films in GHz applications. *International Journal of Microwave and Wireless Technologies* **1**, 19–27.

26. **Bourey N, Darces M, Chatelon Y and Helier M** (2020) Near-field to far-field transformation applied to UHF antennas over lossy ground. *International Journal of Microwave and Wireless Technologies* **12**, 227–232.

27. **Pollayi L, Dasari RK and Pandharipande VM** (2019) Design and development of wide band dual-polarized magneto electric dipole antenna for mobile communications. *International Journal of Microwave and Wireless Technologies* **11**, 175–181.

28. **Wang G, Chen S and Wen J** (2011) Low-frequency locally resonant band gaps induced by arrays of resonant shunts with Antoniou's circuit: experimental investigation on beams. *Smart Materials and Structures* **20**, 015026.

29. **Ruby R, Bradley P and Larson JD** (1999) PCS 1900 MHz duplexer using thin film bulk acoustic resonators. *Electronics Letters* **35**, 794–795.

30. **Zhang H, Xiao Y, Wen J, Yu D and Wen X** (2016) Ultra-thin smart acoustic metasurface for low-frequency sound insulation. *Applied Physics Letters* **108**, 141902.

Yong Zhang was born in Henan Province, China, in 1989. He is currently working towards the Ph.D. degree in electrical engineering with the School of Electrical Engineering, Southwest Jiaotong University, Chengdu, China. His research interests include antenna miniaturization technology and acoustic strain powered antenna technology.
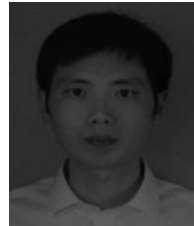
Zhongming Yan was born in Zhejiang Province, China, in 1982. He received the Ph.D. degree in theory of electrical engineering and new technology from Southwest Jiaotong University, Chengdu, China, in 2013. He is currently an associate professor with the School of Electrical Engineering, Southwest Jiaotong University. His research interests include superconducting electromotor and the numerical analysis of electromagnetic fields.

Biao Dong was born in Henan Province, China, in 1999. He is currently working towards the Ph.D. degree in electrical engineering with the School of Electrical Engineering, Southwest Jiaotong University, Chengdu, China. His research interests include antenna miniaturization technology and acoustic strain powered antenna technology.

Yu Wang was born in Henan Province, China, in 1960. He received the Ph.D. degree in physical electronics from the Huazhong University of Science and Technology, Wuhan, China, in 2001. He is currently a professor with the School of Electrical Engineering, Southwest Jiaotong University, Chengdu, China. His research interests include superconducting electrotechnics and material technology.

Hongcheng Zhou was born in Sichuan Province, China, in 1989. She received the Ph.D. degree in electromagnetic fields and microwave technology from University of Electronic Science and Technology of China, Chengdu, China, in 2016. She is currently a lecturer with the School of Electrical Engineering, Southwest Jiaotong University. Her research interests include antenna design and the time reversal electromagnetism.